Article

Estimation of Critical Collapse Solutions to Black Holes with Nonlinear Statistical Models

Ehsan Hatefi and Armin Hatefi

Topic

Data Science and Knowledge Discovery

Edited by
Prof. Dr. Sławomir Nowaczyk, Dr. Rita P. Ribeiro and Prof. Dr. Grzegorz Nalepa

Article

Estimation of Critical Collapse Solutions to Black Holes with Nonlinear Statistical Models

Ehsan Hatefi [1,2,*] and **Armin Hatefi** [3]

1   GRAM Research Group, Department of Signal Theory and Communications, University of Alcala, 28805 Alcala de Henares, Spain
2   Scuola Normale Superiore and I.N.F.N, Piazza dei Cavalieri 7, 56126 Pisa, Italy
3   Department of Mathematics and Statistics, Memorial University of Newfoundland, St. John's, NL A1C 5S7, Canada
*   Correspondence: ehsanhatefi@gmail.com

Abstract: The self-similar gravitational collapse solutions to the Einstein-axion–dilaton system have already been discovered. Those solutions become invariants after combining the spacetime dilation with the transformations of internal $SL(2, R)$. We apply nonlinear statistical models to estimate the functions that appear in the physics of Black Holes of the axion–dilaton system in four dimensions. These statistical models include parametric polynomial regression, nonparametric kernel regression and semi-parametric local polynomial regression models. Through various numerical studies, we reached accurate numerical and closed-form continuously differentiable estimates for the functions appearing in the metric and equations of motion.

Keywords: mathematical physics; black holes; statistical analysis

MSC: 46N55

1. Introduction

As the end state of gravitational collapse, black holes are defined by their mass, angular momentum and their charge. M. Choptuik [1] explored the so-called critical phenomena in gravitational collapse, as well as Choptuik scaling. He made a breakthrough in the subject of numerical relativity. Indeed, Choptuik scaling [1,2] is a property that occurs in various systems that experience gravitational collapse. He discovered that there might be a fourth universal quantity that establishes the critical collapse. Choptuik followed the study of the spherically symmetric collapse of scalar fields and explored a critical behaviour that demonstrates the discrete spacetime self-similarity. By taking the amplitude of the scalar field p, he derived a critical value p_{crit} where a black hole forms as p exceeds p_{crit}. Furthermore, as p goes beyond the threshold, the mass of the black hole M_{bh} illustrates the scaling law

$$M_{\mathrm{bh}}(p) \propto (p - p_{\mathrm{crit}})^{\gamma}, \tag{1}$$

where the Choptuik exponent was found to be $\gamma \simeq 0.37$ [1] in four dimensions and for a real scalar field. Various numerical computations with different matter content have also been discovered [3–7].

Motivated by string theory, the axion–dilaton system can also experience the same gravitational collapse process. The study of the Choptuik phenomenon in the axion–dilaton system was initiated in [8–10]. The AdS/CFT correspondence [11–13] is viewed as the first motivation to investigate critical collapse solutions, especially for the axion–dilaton system. The AdS/CFT correspondence correlates the critical exponent and the imaginary part of quasi normal modes, as well as the dual conformal field theory [14]. The second motivation relies on the holographic description of black hole formation [15], particularly in the physics of black holes and their implications [16–18]. From the IIB string theory point of view, we

look for the gravitational collapse for the special spaces that could asymptotically approach $AdS_5 \times S^5$. The matter field in the IIB string theory arises from the self-dual five-form field strength and the axion–dilaton configuration. In recent research [19,20], the whole families of Continuous Self-Similar (CSS) solutions of the Einstein-axion–dilaton system were explored for all the three conjugacy classes of $SL(2, R)$. Some remarks about critical exponents and higher dimensional solutions have been made in [21,22]. For more details about the other systems experiencing gravitational collapse, readers are referred to [23–27].

To our best knowledge, there is no research article in the literature investigating the properties of nonlinear statistical models to estimate the critical collapse functions in Einstein-axion–dilaton. In this paper, for the first time, we utilise parametric polynomial regression, non-parametric kernel regression and semi-parametric local polynomial regression models to develop a closed form and continuously differentiable functional forms of the critical collapse functions.

This article is organised as follows. We describe the axion–dilaton system and its different continuous self-similar ansatzë in Section 2. The initial conditions and properties of the critical solutions for all three conjugacy classes are discussed in Sections 3 and 4, respectively. The nonlinear statistical estimation methods are then discussed in Section 5. The performance of the proposed statistical models are finally investigated in Section 6. Concluding remarks are presented in Section 7.

2. Axion-Dilaton Configuration

One can combine the axion a and dilaton ϕ field into a single complex field $\tau \equiv a + ie^{-\phi}$, and its coupling to four-dimensional gravity is given by

$$S = \int d^4x \sqrt{-g} \left(R - \frac{1}{2} \frac{\partial_a \tau \partial^a \bar{\tau}}{(\text{Im}\,\tau)^2} \right) . \tag{2}$$

where R is the scalar curvature. The above action describes the effective action of type II string theory [28,29]. This action respects $SL(2, R)$ symmetry, which means that if we consider the following

$$\tau \to \tau \equiv \frac{a\tau + b}{c\tau + d} , \tag{3}$$

the action remains invariant where a, b, c, d are real parameters satisfying $ad - bc = 1$. The equations of motion can be read as follows

$$R_{ab} - \frac{1}{4(\text{Im}\,\tau)^2} (\partial_a \tau \partial_b \bar{\tau} + \partial_a \bar{\tau} \partial_b \tau) = 0 \tag{4}$$

$$\nabla^a \nabla_a \tau + \frac{i \nabla^a \tau \nabla_a \tau}{\text{Im}\,\tau} = 0. \tag{5}$$

We have looked for critical solutions by dealing with spherical symmetry and continuous self-similarity. Following [8–10], one can choose the metric as

$$ds^2 = (1 + u(t,r)) \left(-b(t,r)^2 dt^2 + dr^2 \right) + r^2 d\Omega^2 . \tag{6}$$

We might consider a scale invariant variable as $z \equiv -r/t$, and hence, the continuous self-similarity of the metric actually means that all functions $u(t,r), b(t,r)$ can be expressed just in terms of z, that is, $b(t,r) = b(z), u(t,r) = u(z)$.

This continuous self-similarity condition for τ was described in detail in [30]. The axion–dilaton system does have a global $SL(2, R)$-symmetry, which is broken into an $SL(2, Z)$ by taking into account the non-perturbative phenomena in type II string theory. If we take the quantum effects, $SL(2, R)$ symmetry reduces to $SL(2, Z)$, for which it is believed to be the non-perturbative symmetry of string theory [31–33]. Therefore, one

might compensate the action by means of an $SL(2, R)$-transformation, that is $\tau(t, z)$ must respect the following equation

$$t \frac{\partial}{\partial t} \tau(t, z) = \alpha_0 + \alpha_1 \tau + \alpha_2 \tau^2 \tag{7}$$

with $\alpha_{0,1,2}$ real numbers. The above equation has two roots that are related to compensating the scaling transformation. Having set that, we find three different ansatzë, which are related to the fact that the chosen $SL(2, R)$-transformation is either an elliptic, hyperbolic or parabolic transformation. The elliptic ansatz is defined as

$$\tau(t, r) = i \frac{1 - (-t)^{i\omega} f(z)}{1 + (-t)^{i\omega} f(z)}, \tag{8}$$

where ω is a real constant that will be known by the regularity conditions for the critical solution. On the other hand, for the hyperbolic case, $\tau(t, r)$ is given by

$$\tau(t, r) = \frac{1 - (-t)^\omega f(z)}{1 + (-t)^\omega f(z)}, \tag{9}$$

Eventually the parabolic ansatz is illustrated by $\tau(t, r) = f(z) + \omega \log(-t)$. Note that the function $f(z)$ needs to satisfy $|f(z)| < 1$ for the elliptic case, whereas $\operatorname{Im} f(z) > 0$ for hyperbolic and parabolic cases.

3. Equations of Motion and Initial Conditions

In this section, we first study the equations of motion and then explain the properties of solutions. Replacing CSS into the equations of motion, we derive a system of differential equations just for $b(z), f(z)$. Using Einstein equations for angular variables, one can express $u(z), b(z)$ just in terms of $f(z)$, which means that

$$u(z) = \frac{z\, b'(z)}{b(z)}. \tag{10}$$

Hence, $u(z)$ and its derivatives can be eliminated from equations of motion. The other equations of motion involve $b(z), f(z)$. Hence, we are left with various ordinary differential equations (ODEs)

$$b'(z) = B(b(z), f(z), f'(z)), \tag{11}$$
$$f''(z) = F(b(z), f(z), f'(z)). \tag{12}$$

Since, in this paper, we are looking for an estimation of the function of $b(z)$ and real and imaginary parts of $f(z)$ for elliptic and hyperbolic cases in four dimensions, we just generate those equations as follows. Indeed, the equations of motion are derived in [30]. The equations for the elliptic case are

$$
\begin{aligned}
0 = {}& b' + \frac{z(b^2 - z^2)}{b(-1 + |f|^2)^2} f' \bar{f}' - \frac{i\omega(b^2 - z^2)}{b(-1 + |f|^2)^2}(f\bar{f}' - \bar{f}f') - \frac{\omega^2 z|f|^2}{b(-1 + |f|^2)^2}, \\
0 = {}& f'' - \frac{z(b^2 + z^2)}{b^2(-1 + |f|^2)^2} f'^2 \bar{f}' + \frac{2}{(1 - |f|^2)}\left(1 - \frac{i\omega(b^2 + z^2)}{2b^2(1 - |f|^2)}\right)\bar{f}f'^2 \\
& + \frac{i\omega(b^2 + 2z^2)}{b^2(-1 + |f|^2)^2} ff'\bar{f}' + \frac{2}{z}\left(1 + \frac{i\omega z^2(1 + |f|^2)}{(b^2 - z^2)(1 - |f|^2)}\right. \\
& \left. + \frac{\omega^2 z^4 |f|^2}{b^2(b^2 - z^2)(1 - |f|^2)^2}\right)f' + \frac{\omega^2 z}{b^2(-1 + |f|^2)^2} f^2 \bar{f}' + \\
& \frac{2i\omega}{(b^2 - z^2)}\left(\frac{1}{2} - \frac{i\omega(1 + |f|^2)}{2(1 - |f|^2)} - \frac{\omega^2 z^2 |f|^2}{2b^2(-1 + |f|^2)^2}\right)f.
\end{aligned}
\tag{13}
$$

Using time scaling, one can set $b(t, 0) = 1$. In the elliptic case, by writing $f(z) = f_m(z)e^{if_a(z)}$, the regularity conditions imply:

$$
b(0) = 1, f_m'(0) = f_a'(0) = 0
\tag{14}
$$

The above equations are invariant under a global phase of $f(z)$, so we can choose

$$
f_a(0) = 0
\tag{15}
$$

For a hyperbolic case, the equations are determined by

$$
\begin{aligned}
0 = {}& b' - \frac{z(b^2 - z^2)}{b(f - \bar{f})^2} f'\bar{f}' + \frac{\omega(b^2 - z^2)}{b(f - \bar{f})^2}(f\bar{f}' + \bar{f}f') + \frac{\omega^2 z|f|^2}{b(f - \bar{f})^2} \\
0 = {}& -f'' - \frac{z(b^2 + z^2)}{b^2(f - \bar{f})^2} f'^2 \bar{f}' + \frac{2}{(f - \bar{f})}\left(\frac{1}{\bar{f}} + \frac{\omega(b^2 + z^2)}{2b^2(f - \bar{f})}\right)\bar{f}f'^2, \\
& + \frac{\omega(b^2 + 2z^2)}{b^2(f - \bar{f})^2} ff'\bar{f}' + \frac{2}{z}\left(-1 + \frac{\omega z^2(f + \bar{f})}{(b^2 - z^2)(f - \bar{f})}\right. \\
& \left. + \frac{\omega^2 z^4 |f|^2}{b^2(b^2 - z^2)(f - \bar{f})^2}\right)f' - \frac{\omega^2 z}{b^2(f - \bar{f})^2} f^2 \bar{f}' + \\
& \frac{2\omega}{(b^2 - z^2)}\left(-\frac{1}{2} - \frac{\omega(f + \bar{f})}{2(f - \bar{f})} - \frac{\omega^2 z^2 |f|^2}{2b^2(f - \bar{f})^2}\right)f.
\end{aligned}
\tag{16}
$$

They are invariant under a constant scaling $f \to \lambda f$, and applying regularity at the origin, we find that $f'(z = 0)$ should vanish. Thus, the initial conditions for the hyperbolic case are:

$$
b(0) = 1, f'(0) = 0
\tag{17}
$$

Finally, in the parabolic ansatz, the equations of motion are invariant under arbitrary shifts of $f(z)$.

4. Properties of the Critical Solutions

The properties of the solutions and the physical and geometrical behaviours of the solutions for the elliptic case are explained in detail in [9,10]. Naturally, for the hyperbolic case, the same properties are being held. In all equations, we have five singularities where $z = \pm 0$ corresponds to the origin, and we have dealt with them by making the regularity conditions. On the other hand, the point $z = \infty$ related to $t = 0$. By the change in variables and redefinition of the fields $f(z), b(z)$, one can show that [34] the equations remain regular there as well.

The singularities $b(z_\pm) = \pm z_\pm$ are the locations where the homothetic killing vector is null, as explained in [30]. For $b(z_+) = z_+$, the solution must be smooth within this surface, and we need to have the continuity of f, b in this region. $b(z_+) = z_+$ is related to the homothetic horizon, and it is indeed a mere coordinate singularity [30,35], so τ must be finite across it, which becomes interpreted as the finiteness of $f''(z)$ once $z \to z_+$. Another constraint comes from the fact that the vanishing of the divergent part of $f''(z)$ generates one complex valued constraint at z_+ that can be defined by $G(b(z_+), f(z_+), f'(z_+)) = 0$, where the definitions of G are given in Equations (49)–(51) of [19]. If we use regularity at $z = 0$, as well as the residual symmetries, then we find out the initial conditions $b(0) = 1, f'(0) = 0$ and the value of $f(0)$ is shown by

$$f(0) = \begin{cases} x_0 & \text{elliptic} & (0 < x_0 < 1) \\ ix_0 & \text{parabolic} & (0 < x_0) \\ 1 + ix_0 & \text{hyperbolic} & (0 < x_0) \end{cases} \tag{18}$$

where x_0 is a real parameter. Thus, we have two constraints as the real and imaginary parts of G must be vanished and two parameters (ω, x_0) are to be known.

The entire solutions for the hyperbolic case in four and five dimensions have been derived in [20]. These solutions are obtained by making use of numerical integration from the equations of motion. For instance, for four-dimensional elliptic cases, just one solution is determined [10,30], and it is given by

$$\begin{aligned} \omega &= 1.176, \\ z_+ &= 2.605, \\ |f(0)| &= 0.892, \end{aligned} \tag{19}$$

Using this new search methodology, we are able to explore the entire families of solutions for the hyperbolic case in four dimensions, which are three cases called α, β, γ solutions. The α solution is given by

$$\omega = 1.362, \quad z_+ = 1.440, \quad \text{Im } f(0) = 0.708. \tag{20}$$

The β solution is determined by

$$\omega = 1.003, \quad z_+ = 3.29, \quad \text{Im } f(0) = 0.0822. \tag{21}$$

Finally, the γ solution is explored to be

$$\omega = 0.541, \quad z_+ = 8.44, \quad \text{Im } f(0) = 0.0059. \tag{22}$$

5. Statistical Estimation Methods

Throughout this section, we use the following notations to present the statistical estimation methods. Let $(\mathbf{X}, \mathbf{y})$ denote a multivariate random variable from a random sample of size n. Suppose $\mathbf{y} = (y_1 \dots, y_n)$ and $\mathbf{X} = (\mathbf{x}_1, \dots, \mathbf{x}_p)$ represent, respectively, the vector of response variable of size n and $(n \times p)$ dimensional design matrix with p explanatory variables, where $\text{rank}(\mathbf{X}) = p < n$.

5.1. Polynomial Regression Model

Linear regression models are among the most popular statistical methods for modelling data. One can address the relationship between response variable y and the explanatory variables $\mathbf{x}_1, \dots, \mathbf{x}_p$ by the linear regression model

$$y_i = x_i^\top \beta + \epsilon_i, \quad i = 1, \dots, n, \tag{23}$$

where β is the unknown parameters (hence-after called coefficients) of the model, $x_i^\top$ indicates the transpose of x_i and that $\epsilon_i \overset{iid}{\sim} N(0,1); i = 1, \ldots, n$; that is, the error terms are independent and identically distributed from standard normal distribution [36].

It is easily seen that linear regression model (23), as a parametric method, translates the prediction problem of the response function $y = g(x)$ (as a function of explanatory variable x) to the estimation problem of the unknown parameters/coefficients of the model. The least square (LS) method [36] is one of the most common approaches to estimating the coefficients of model (23). Given the design matrix $\mathbf{X}$ and response vector $\mathbf{y}$ from n observations, the least squares estimate of β is given by

$$\widehat{\beta}_{LS} = \arg\min_{\beta} ||\mathbf{y} - \mathbf{X}\beta||_2^2, \tag{24}$$

where $|| \cdot ||_2^2$ denotes the l_2 norm. It is easy to show that the solution to (24) is given by

$$\widehat{\beta}_{LS} = (\mathbf{X}^\top\mathbf{X})^{-1}\mathbf{X}^\top\mathbf{y}. \tag{25}$$

Once model (23) is trained, the response can be predicted at a new value x_{new} by

$$\widehat{y}_{new} = \widehat{g}(x_{new}) = x_{new}^\top\widehat{\beta}_{LS}. \tag{26}$$

It is evident that the functional forms of $|f_0(z)|$, $\arg(f_0(z))$ and $b_0^2(z) - z^2$, as our underlying statistical population to be estimated, are clearly nonlinear functions of space-time. Hence, the simple linear regression model (23) based on z is not flexible enough to estimate the nonlinearity of critical collapse functions. One can employ a polynomial regression model to deal with the nonlinear critical collapse functions. The polynomial regression model enables us to incorporate the higher orders of explanatory variable x to better approximate the nonlinear response function $y = g(x)$. A polynomial regression model of order l is given by

$$y_i = \sum_{j=0}^{l} x_i^j \beta_j + \epsilon_i, \tag{27}$$

where $\beta = (\beta_0, \ldots, \beta_l)$ represent the unknown coefficients of the model. Note that we only focus on the main effects of explanatory variables (and their higher orders) in estimating the critical functions. First, in the estimating of the critical functions, there is only a single explanatory variable, that is, the spacetime z. Hence, no interaction term is defined in the regression models. When there is a single explanatory variable in the regression, the higher orders of the explanatory variable can very well accommodate the nonlinearity of the population. Finally, the interaction terms typically contribute to the refinement of the estimates at the price of introducing more parameters in the model and reducing the degree of freedom in the estimation. For the above reasons, throughout this manuscript, we do not include the interaction terms in the statistical models.

The polynomial regression model, as a special case of model (23), can be written as a linear model again by

$$\mathbf{y} = \mathbf{Z}\beta + \epsilon,$$

where the columns of matrix $\mathbf{Z}$ are the copies of explanatory variable x_i taken to various powers $j = 0, \ldots, l$. Similarly, from the least squares method (24), the polynomial regression at x_{new} is produced by

$$\widehat{y}_{new} = \widehat{g}(x_{new}) = x_{new}^\top(\mathbf{Z}^\top\mathbf{Z})^{-1}\mathbf{Z}^\top\mathbf{y}. \tag{28}$$

The polynomial regression model provides a flexible solution to estimate a nonlinear function at the price of higher orders of explanatory variable x in the model. Therefore, the

estimation performance of the polynomial proposal depends on the order of the polynomial regression l. In Section 6, we perform a cross validation to select the best order of the polynomial estimators.

5.2. Kernel Regression Model

Linear regression and polynomial regression models translate the estimation problem of the response function $y = g(x)$ to the estimation problem of parameters β. Non-parametric regression models can be considered as another approach to estimate the nonlinear critical collapse functions. A kernel regression model is one of the most common non-parametric estimation methods. Kernel regression approximates the response function at new observation x_{new} by a weighted average of observed responses in a neighbourhood of x_{new}. A kernel function is non-negative symmetric function around the origin (i.e., the centre of the neighbourhood). Kernel function is typically re-scaled to result in a legitimate probability density function in each neighbourhood. There are various choices for the kernel function; however, in this manuscript, we focus only on Epanechnikov kernel [37] given by

$$K_h(x) = 3/4\Big(1 - (x/h)^2\Big)I\big(|x/h| \le 1\big), \tag{29}$$

where h denotes the bandwidth parameter of the kernel function K. and I is an indicator function such that $I(u) = 1$ if u=true otherwise $I(u) = 0$. It is at once apparent that the kernel function (29) tunes the width of neighbourhoods based on the bandwidth parameter h. When an observation falls out of the bandwidth, the kernel function assigns a very small weight to the observation to reduce its impact on the function estimate.

Given a training data set of size n with explanatory variable x and response y, the Nadaraya–Watson kernel regression estimates [38,39] the response function at new observation x_{new} as

$$\widehat{y}_{new} = \widehat{g}(x_{new}) = \sum_{i=1}^{n} \frac{K_h(|x_i - x_{new}|)y_i}{\sum_{r=1}^{n} K_h(|x_r - x_{new}|)}, \tag{30}$$

where $K_h(\cdot)$ is obtained from (29).

Note that the kernel regression estimator (30) deals with the nonlinearity of response function at the price of selecting the bandwidth parameter. To this end, when small h is selected, the weights assigned by kernel regression estimator are more concentrated around the new observation (i.e., shorter neighbourhoods will be declared). In contrast, when large h is selected, the weights will be more spread out and, consequently, wider neighbourhoods are declared. Hence, for a piece of given training data, we carry out a cross validation to find out the optimal bandwidth.

5.3. Local Regression Model

As another approach, we study the local regression model to earn the curvature of the response function $y = g(x)$. Local regression, as a semi-parametric approach, combines the parametric advantages of the polynomial regression and non-parametric properties of the kernel regression in estimating the response function. Local regression can be intuitively explained by the Taylor expansion of $g(x)$ around x_{new} as follows:

$$g(x_{new} + \delta) = g(x_{new}) + \delta\frac{\partial g}{\partial x}(x_{new}) + \frac{\delta^2}{2}\frac{\partial^2 g}{\partial x^2}(x_{new}) + O(\delta^3),$$

where kernel regression can be viewed as an estimator that only utilises the constant term to approximate $g(x)$. The local regression method exploits the high orders of x by polynomial regression and then estimates the coefficients (of the polynomial regression) by the kernel regression in each neighbourhood.

Given a training data set of size n with explanatory variable x and response variable y, the local regression estimator [37] of order l at x_{new} is given by

$$\widehat{y}_{\text{new}} = \widehat{g}(x_{\text{new}}) = \sum_{j=0}^{l} x_i^j \widehat{\beta}_j(x_{\text{new}}), \tag{31}$$

where the vector of coefficients estimate $\widehat{\beta}(x_{\text{new}}) = \left(\widehat{\beta_0}(x_{\text{new}}), \dots, \widehat{\beta_l}(x_{\text{new}}) \right)$ is obtained as a solution to:

$$\widehat{\beta}(x_{\text{new}}) = \arg\min_{\beta} \left\{ \sum_{i=1}^{n} K_h(|x_i - x_{\text{new}}|) \left(y_i - \sum_{j=0}^{l} x_i^j \beta_j \right)^2 \right\}, \tag{32}$$

where $K_h(\cdot)$ obtained from (29).

The estimator (31) can be used to estimate the response function at any value of x_{new}. Accordingly, the estimator (31) enables us to approximate the response function $y = g(x)$ throughout the domain. Note that the local regression smoother (31) requires two tuning parameters. These tuning parameters include the bandwidth parameter of kernel part h and the order of the polynomial part l.

6. Numerical Studies

R. Antonelli and E. Hatefi in [19] recently studied the black hole solutions of an axion–dilaton system in elliptic and hyperbolic cases in four and five dimensions. Through the numerical optimisation of [10], they found only one solution to equations of motion for four dimensions of elliptic cases. As discussed in [20], the unperturbed critical collapse functions play a key role in the location of the critical solutions and critical exponents. Despite the importance of these unperturbed critical collapse functions, little information is known in the literature about the structure and closed form of these functions. It is, thus, of high importance for researchers to numerically estimate the functional form of these unperturbed functions so that the critical solutions and critical exponents, as well as the mass of black holes and universality of Choptuik exponents, will be more tractable. In this section, we employ nonlinear statistical methods, including polynomial regression, non-parametric kernel regression and local polynomial regression methods to estimate the functional forms of the unperturbed critical collapse functions.

Using the optimisation techniques of [10], a numerical search is carried out to find the critical solution on various intervals in the domain of forward singularity ($[0, z_+]$). Accordingly, they showed that there was a unique critical solution in elliptic space. This results in the interval $[0, 2.5]$ as the domain of the critical collapse functions in elliptic space in four dimensions, where this unique solution was also confirmed in [19]. Similarly, R. Antonelli and E. Hatefi [19] explored three solutions (say α, β and γ critical solutions) to the equation of motion in the hyperbolic case. This leads to three corresponding domains, including $[0, 1.44]$, $[0, 3.30]$ and $[0, 8.45]$ for the unperturbed functions. In a similar vein to [19], we carried out the optimisation search and obtained 2000 observations from the critical functions $b_0^2 - z^2$, $|f_0|$ and $\arg f_0$ in all elliptic and hyperbolic domains. These observations were treated as the (unknown) underlying statistical populations to be estimated.

For each observation in the population, we generated four characteristics from the valid domain of unperturbed critical solutions of $[0, z_+]$. These characteristics include the realisations of critical functions $b_0^2 - z^2$, $|f_0|$, $\arg f_0$ and z. In the statistical analysis, we considered spacetime z as the single explanatory variable (x) and the realisation of the critical collapse functions $b_0^2 - z^2$, $|f_0|$, $\arg f_0$ as the responses (observed from the corresponding critical function) in the regression models. We fitted one regression model for each critical function. We independently generated (i.e., with replacement) training samples of size $n = 100$ from each population. For the validation of the estimation, we generated (independent from the training data) test data (x_{test}, y_{test}) of size $n = 100$ from

the entire domains of the critical functions. As described in Section 5, to estimate the critical function by the polynomial regression, we first applied Equation (25) to the training data and estimated the coefficients of the model. Using the estimated coefficients $\widehat{\beta}$ and (26), we then predicted the response of the critical function $(\widehat{y}_{test})$ at x_{test}. For the Kernel regression method, we applied Equation (30) to the training data and predicted the value of the critical function $(\widehat{y}_{test})$ at test point x_{test}. According to the definition of the local regression, the coefficients of the model are treated as the functions of the test data. Hence, we used the training data and estimated the coefficients using (32). From (31) and the estimated the coefficients $\widehat{\beta}(x_{test})$, we then predicted the critical collapse function $(\widehat{y}_{test})$ at x_{test}. We finally implemented the above prediction procedures sequentially for all the points in the test data to estimate all the critical collapse functions over their entire domains.

To assess the accuracy of the proposed estimators, we used the measure of square root of the mean squared errors $\sqrt{\text{MSE}}$ as follows

$$\sqrt{\text{MSE}} = \left(1/n \sum_{i=1}^{n} (\widehat{y}_{test,i} - y_{test,i}) \right)^{1/2},$$

Note that the trained model will be more accurate in estimating the critical collapse response function when $\sqrt{\text{MSE}}$ is small. To investigate the impact of tuning parameters on the performance of the estimators, similar to above, we generated training data and validation data of sizes $n = 100$ from the population and computed the $\sqrt{\text{MSE}}$s of estimates of critical collapse functions for $h = \{0.01, 0.02, \ldots, 0.5\}$ and $l = \{1, 2, \ldots, 10\}$.

Tables 1–9 show the results of the numerical studies for all $l = 1, \ldots, 10$ and the top ten h values. It is at once apparent that all the proposed estimators (excluding the polynomial of order $l = 1$) perform very well in predicting the critical collapse functions in all elliptic and hyperbolic domains. The $\sqrt{\text{MSE}}$s of estimators are very small such that the polynomial regression, kernel regression, and local regression estimators can be considered almost unbiased in the estimation of critical collapse functions even in the neighbourhood of the critical singularities. For a graphical comparison of the proposed methods in estimating the critical functions, we presented the performance of the estimates in Figures 1–12 for each combination of the statistical methods, critical collapse functions and spaces. For example, Figure 1 shows the performance of the local regression model in estimating the critical collapse functions. The best performance of the local estimate appeared when h was between $(0.07, 0.08)$; however, we intentionally selected more widely spaced h vales, namely $0.07, 0.10, 0.25, 0.5, 0.75, 1.0$ so that the human eyes can visually distinguish the curves. From Figure 1, it is clear the h values greater than 0.10 result in over-smoothed estimates and consequently the prediction error increases. From Figures 3–5, one can graphically compare the performance of polynomial, kernel and local regression models in estimating the critical functions in elliptic space. From Figures 1, 2 and 6, one can graphically compare the performance of the proposed models in estimating the critical functions corresponding to α-solution of the hyperbolic space. From Figures 7–9, we can graphically compare the performance of the proposed statistical models in estimating the critical functions corresponding to the β-solution of the hyperbolic space. From Figures 10–12, we can, finally, graphically compare the performance of the statistical models in estimating the critical functions corresponding to the γ-solution of the hyperbolic space.

Table 1. The $\sqrt{\text{MSE}}$ of local regression method with $l = 1$ and bandwidth h (presented in parenthesis) in estimating the critical collapse response function $g(z) = b_0^2(z) - z^2$ in elliptic and hyperbolic cases based on a training sample of size $n = 100$.

Elliptic	Hyperbolic		
	α-Solution	β-Solution	γ-Solution
0.00370 (0.10)	0.00040 (0.060)	0.00681 (0.140)	0.13307 (0.29)
0.00438 (0.11)	0.00043 (0.062)	0.00702 (0.142)	0.13375 (0.30)
0.00521 (0.12)	0.00045 (0.064)	0.00723 (0.144)	0.13450 (0.31)
0.00608 (0.13)	0.00048 (0.066)	0.00743 (0.146)	0.13532 (0.32)
0.00693 (0.14)	0.00050 (0.068)	0.00763 (0.148)	0.13909 (0.33)
0.00780 (0.15)	0.00053 (0.070)	0.00782 (0.150)	0.14370 (0.34)
0.00870 (0.16)	0.00055 (0.072)	0.00801 (0.152)	0.14677 (0.35)
0.00980 (0.17)	0.00058 (0.074)	0.00820 (0.154)	0.14910 (0.36)
0.01093 (0.18)	0.00060 (0.076)	0.00839 (0.156)	0.15134 (0.37)
0.01203 (0.19)	0.00063 (0.078)	0.00861 (0.158)	0.15342 (0.38)

Table 2. The $\sqrt{\text{MSE}}$ of local regression method with $l = 1$ and bandwidth h (presented in parenthesis) in estimating the critical collapse response function $g(z) = |f_0(z)|$ in elliptic and hyperbolic cases based on a training sample of size $n = 100$.

Elliptic	Hyperbolic		
	α-Solution	β-Solution	γ-Solution
0.00052 (0.10)	0.00021 (0.060)	0.00024 (0.140)	0.00005 (0.29)
0.00059 (0.11)	0.00022 (0.062)	0.00025 (0.142)	0.00006 (0.30)
0.00069 (0.12)	0.00024 (0.064)	0.00025 (0.144)	0.00006 (0.31)
0.00080 (0.13)	0.00025 (0.066)	0.00026 (0.146)	0.00006 (0.32)
0.00090 (0.14)	0.00026 (0.068)	0.00027 (0.148)	0.00006 (0.33)
0.00099 (0.15)	0.00027 (0.070)	0.00027 (0.150)	0.00006 (0.34)
0.00109 (0.16)	0.00028 (0.072)	0.00028 (0.152)	0.00006 (0.35)
0.00121 (0.17)	0.00029 (0.074)	0.00028 (0.154)	0.00006 (0.36)
0.00132 (0.18)	0.00030 (0.076)	0.00029 (0.156)	0.00006 (0.37)
0.00143 (0.19)	0.00031 (0.078)	0.00029 (0.158)	0.00006 (0.38)

Table 3. The $\sqrt{\text{MSE}}$ of local regression method with $l = 1$ and bandwidth h (presented in parenthesis) in estimating the critical collapse response function $g(z) = \arg f_0(z)$ in elliptic and hyperbolic cases based on a training sample of size $n = 100$.

Elliptic	Hyperbolic		
	α-Solution	β-Solution	γ-Solution
0.00020 (0.10)	0.00026 (0.060)	0.00074 (0.140)	0.00138 (0.29)
0.00024 (0.11)	0.00028 (0.062)	0.00077 (0.142)	0.00138 (0.30)
0.00028 (0.12)	0.00030 (0.064)	0.00079 (0.144)	0.00138 (0.31)
0.00032 (0.13)	0.00032 (0.066)	0.00082 (0.146)	0.00138 (0.32)
0.00037 (0.14)	0.00034 (0.068)	0.00084 (0.148)	0.00140 (0.33)
0.00041 (0.15)	0.00036 (0.070)	0.00086 (0.150)	0.00143 (0.34)
0.00047 (0.16)	0.00037 (0.072)	0.00088 (0.152)	0.00145 (0.35)
0.00053 (0.17)	0.00039 (0.074)	0.00090 (0.154)	0.00146 (0.36)
0.00060 (0.18)	0.00041 (0.076)	0.00092 (0.156)	0.00147 (0.37)
0.00067 (0.19)	0.00043 (0.078)	0.00094 (0.158)	0.00148 (0.38)

Table 4. The $\sqrt{\text{MSE}}$ of polynomial regression method of orders $l = 1, \ldots, 10$ in estimating the critical collapse response function $g(z) = b_0^2(z) - z^2$ in elliptic and hyperbolic cases based on a training sample of size $n = 100$.

l	Elliptic	Hyperbolic		
		α-Solution	β-Solution	γ-Solution
1	0.7063268	0.0819795	1.0307328	6.3570261
2	0.0559801	0.0029784	0.0726698	0.5711519
3	0.0548808	0.0024525	0.0459405	0.2627902
4	0.0334353	0.0003811	0.0432772	0.1278611
5	0.0174070	0.0002913	0.0294283	0.0666275
6	0.0066110	0.0001207	0.0155586	0.0428675
7	0.0019199	0.0000196	0.0077121	0.0315803
8	0.0006227	0.0000030	0.0033251	0.0210668
9	0.0006231	0.0000026	0.0012466	0.0125086
10	0.0004316	0.0000018	0.0004576	0.0080795

Table 5. The $\sqrt{\text{MSE}}$ of polynomial regression method of orders $l = 1, \ldots, 10$ in estimating the critical collapse response function $g(z) = |f_0(z)|$ in elliptic and hyperbolic cases based on a training sample of size $n = 100$.

l	Elliptic	Hyperbolic		
		α-Solution	β-Solution	γ-Solution
1	0.0519709	0.0188249	0.0073093	0.0044686
2	0.0118848	0.0092961	0.0051240	0.0012997
3	0.0056050	0.0054771	0.0042886	0.0002376
4	0.0053751	0.0020169	0.0021204	0.0000318
5	0.0039364	0.0001069	0.0008176	0.0000250
6	0.0020805	0.0001055	0.0002720	0.0000202
7	0.0009439	0.0000180	0.0002590	0.0000148
8	0.0002851	0.0000179	0.0002272	0.0000092
9	0.0000928	0.0000055	0.0001656	0.0000047
10	0.0000915	0.0000043	0.0000998	0.0000027

Table 6. The $\sqrt{\text{MSE}}$ of polynomial regression method of orders $l = 1, \ldots, 10$ in estimating the critical collapse response function $g(z) = \arg f_0(z)$ in elliptic and hyperbolic cases based on a training sample of size $n = 100$.

l	Elliptic	Hyperbolic		
		α-Solution	β-Solution	γ-Solution
1	0.0191634	0.0415803	0.0441231	0.0190365
2	0.0124265	0.0200282	0.0151237	0.0046392
3	0.0044581	0.0041933	0.0049122	0.0017751
4	0.0011409	0.0011059	0.0043728	0.0008067
5	0.0009282	0.0006399	0.0037591	0.0004130
6	0.0007546	0.0000730	0.0024571	0.0002704
7	0.0004682	0.0000358	0.0014501	0.0002036
8	0.0001987	0.0000206	0.0007639	0.0001393
9	0.0000671	0.0000197	0.0003697	0.0000851
10	0.0000268	0.0000113	0.0001545	0.0000566

Table 7. The $\sqrt{\text{MSE}}$ of kernel regression method evaluated at bandwidth h (presented in parenthesis) in estimating the critical collapse response function $g(z) = b_0^2(z) - z^2$ in elliptic and hyperbolic cases based on a training sample of size $n = 100$.

| Elliptic | Hyperbolic | | |
	α-Solution	β-Solution	γ-Solution
0.03150 (0.06)	0.00531 (0.042)	0.05777 (0.110)	0.45314 (0.20)
0.03291 (0.07)	0.00525 (0.044)	0.05781 (0.112)	0.46026 (0.21)
0.03414 (0.08)	0.00524 (0.046)	0.05783 (0.114)	0.44735 (0.22)
0.03359 (0.09)	0.00527 (0.048)	0.05775 (0.116)	0.43467 (0.23)
0.03413 (0.10)	0.00525 (0.050)	0.05767 (0.118)	0.43196 (0.24)
0.03585 (0.11)	0.00528 (0.052)	0.05761 (0.120)	0.43750 (0.25)
0.03823 (0.12)	0.00537 (0.054)	0.05764 (0.122)	0.45320 (0.26)
0.04059 (0.13)	0.00539 (0.056)	0.05777 (0.124)	0.47516 (0.27)
0.04272 (0.14)	0.00539 (0.058)	0.05775 (0.126)	0.49798 (0.28)
0.04479 (0.15)	0.00539 (0.060)	0.05767 (0.128)	0.51837 (0.29)

Table 8. The $\sqrt{\text{MSE}}$ of kernel regression method evaluated at bandwidth h (presented in parenthesis) in estimating the critical collapse response function $g(z) = |f_0(z)|$ in elliptic and hyperbolic cases based on a training sample of size $n = 100$.

| Elliptic | Hyperbolic | | |
	α-Solution	β-Solution	γ-Solution
0.00324 (0.06)	0.00088 (0.032)	0.00227 (0.07)	0.00088 (0.20)
0.00346 (0.07)	0.00088 (0.034)	0.00230 (0.08)	0.00086 (0.21)
0.00339 (0.08)	0.00087 (0.036)	0.00240 (0.09)	0.00082 (0.22)
0.00342 (0.09)	0.00087 (0.038)	0.00248 (0.10)	0.00078 (0.23)
0.00350 (0.10)	0.00085 (0.040)	0.00250 (0.11)	0.00075 (0.24)
0.00380 (0.11)	0.00085 (0.042)	0.00249 (0.12)	0.00072 (0.25)
0.00411 (0.12)	0.00086 (0.044)	0.00250 (0.13)	0.00070 (0.26)
0.00437 (0.13)	0.00087 (0.046)	0.00249 (0.14)	0.00070 (0.27)
0.00452 (0.14)	0.00090 (0.048)	0.00248 (0.15)	0.00070 (0.28)
0.00471 (0.15)	0.00092 (0.050)	0.00255 (0.16)	0.00072 (0.29)

Table 9. The $\sqrt{\text{MSE}}$ of kernel regression method evaluated at bandwidth h (presented in parenthesis) in estimating the critical collapse response function $g(z) = \arg f_0(z)$ in elliptic and hyperbolic cases based on a training sample of size $n = 100$.

| Elliptic | Hyperbolic | | |
	α-Solution	β-Solution	γ-Solution
0.00273 (0.06)	0.00379 (0.024)	0.00742 (0.10)	0.00397 (0.20)
0.00293 (0.07)	0.00379 (0.026)	0.00725 (0.11)	0.00403 (0.21)
0.00307 (0.08)	0.00350 (0.028)	0.00709 (0.12)	0.00392 (0.22)
0.00310 (0.09)	0.00352 (0.030)	0.00705 (0.13)	0.00378 (0.23)
0.00309 (0.10)	0.00356 (0.032)	0.00699 (0.14)	0.00373 (0.24)
0.00316 (0.11)	0.00366 (0.034)	0.00688 (0.15)	0.00376 (0.25)
0.00323 (0.12)	0.00374 (0.036)	0.00697 (0.16)	0.00387 (0.26)
0.00333 (0.13)	0.00379 (0.038)	0.00714 (0.17)	0.00405 (0.27)
0.00344 (0.14)	0.00373 (0.040)	0.00745 (0.18)	0.00424 (0.28)
0.00356 (0.15)	0.00364 (0.042)	0.00801 (0.19)	0.00439 (0.29)
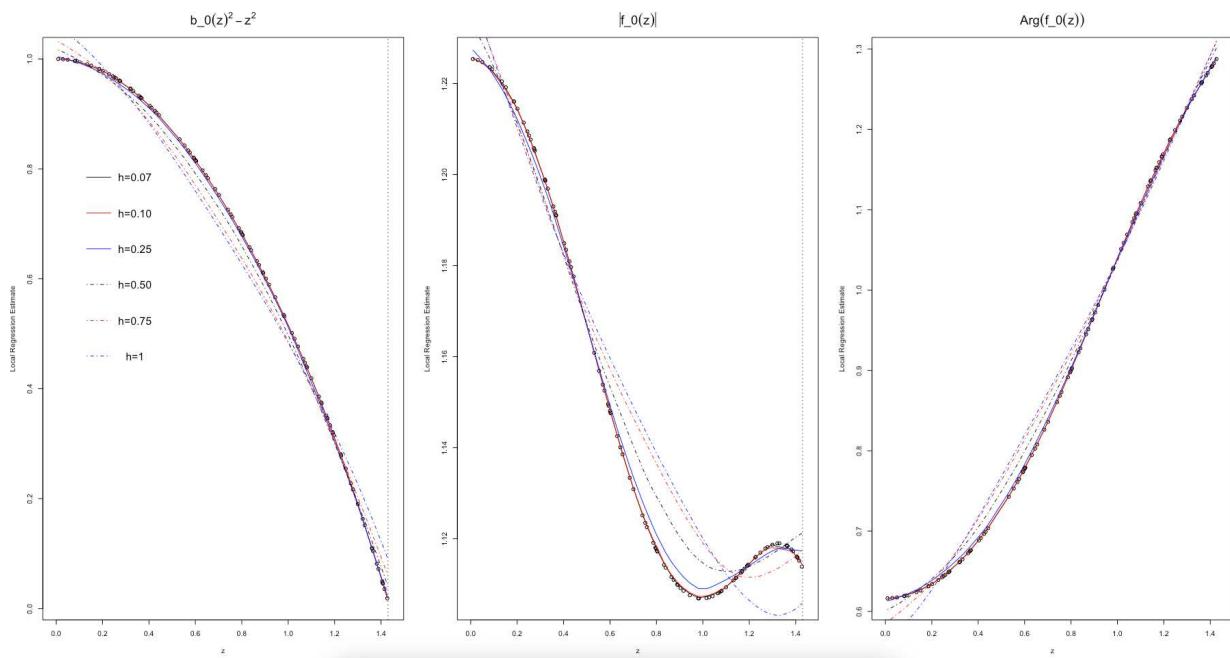
Figure 1. The estimates of critical collapse functions corresponding to α solution of hyperbolic case based on a local regression method of order $l = 1$ with bandwidth parameters $h = \{0.07, 0.10, 0.25, 0.50, 0.75, 1\}$ based on a training sample of size $n = 100$.
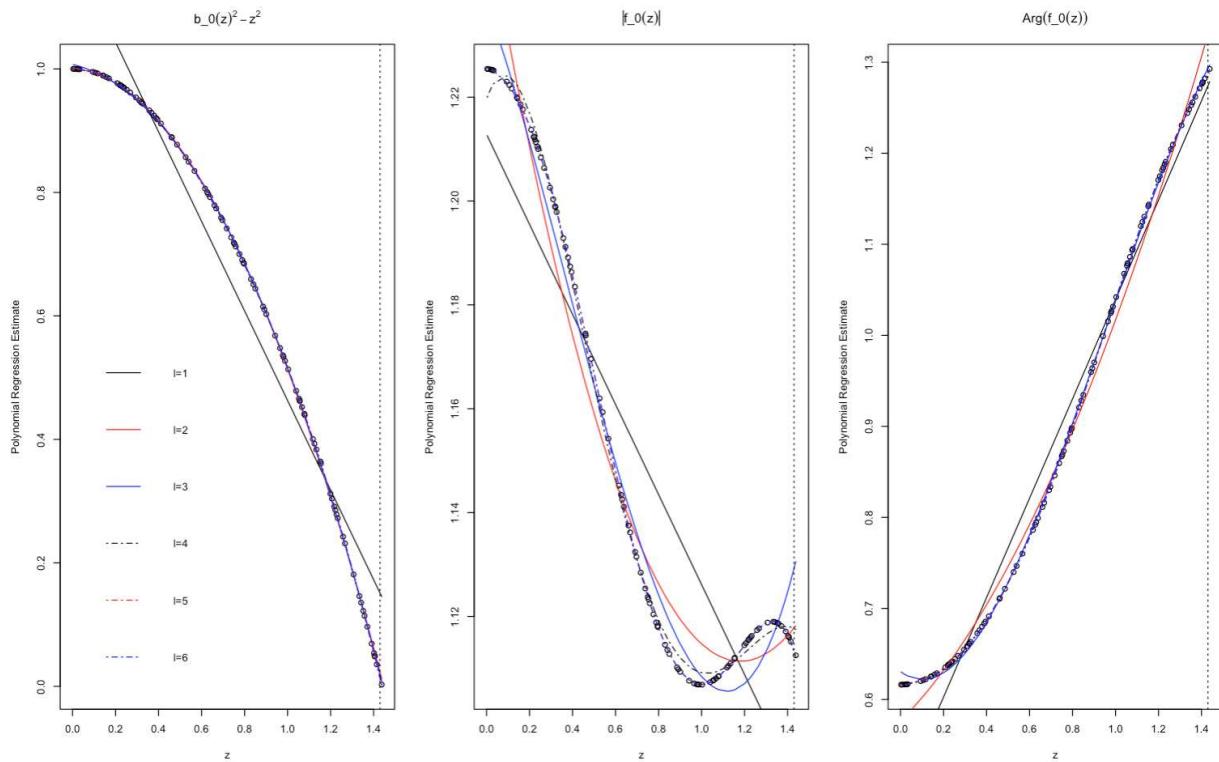

Figure 2. The estimates of critical collapse functions corresponding to α solution of hyperbolic case based on a polynomial regression method of orders $l = \{1, \ldots, 6\}$ based on a training sample of size $n = 100$.
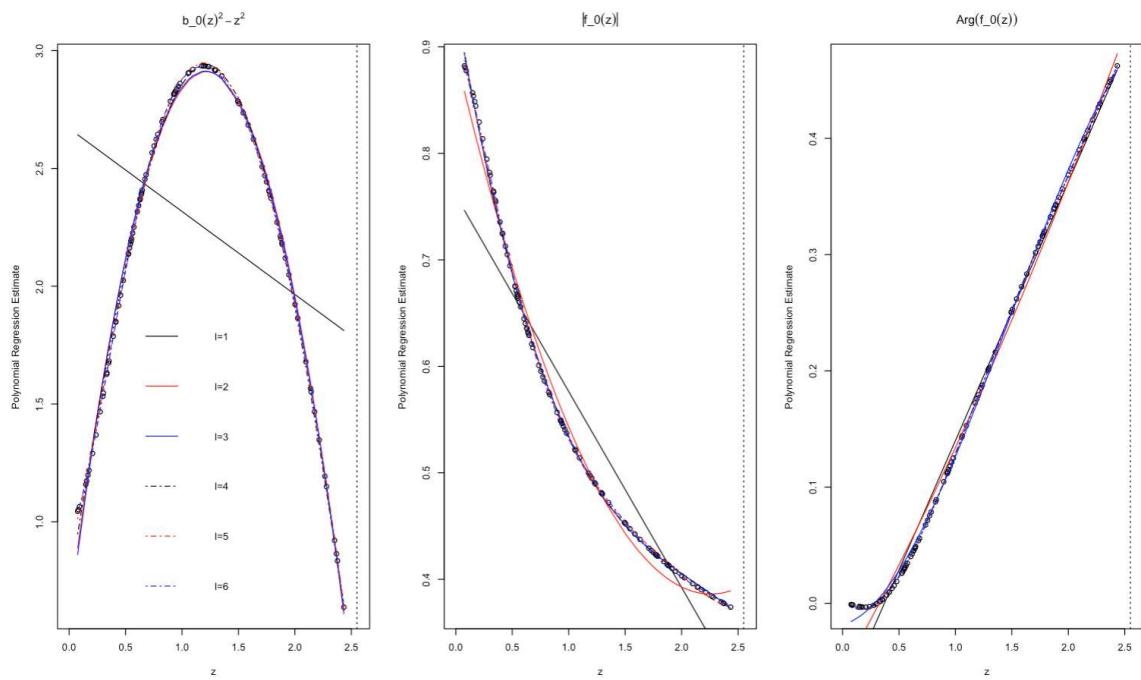
Figure 3. The estimates of critical collapse functions based on a polynomial regression method of orders $l = \{1, \ldots, 6\}$ in elliptic case based on a training sample of size $n = 100$.
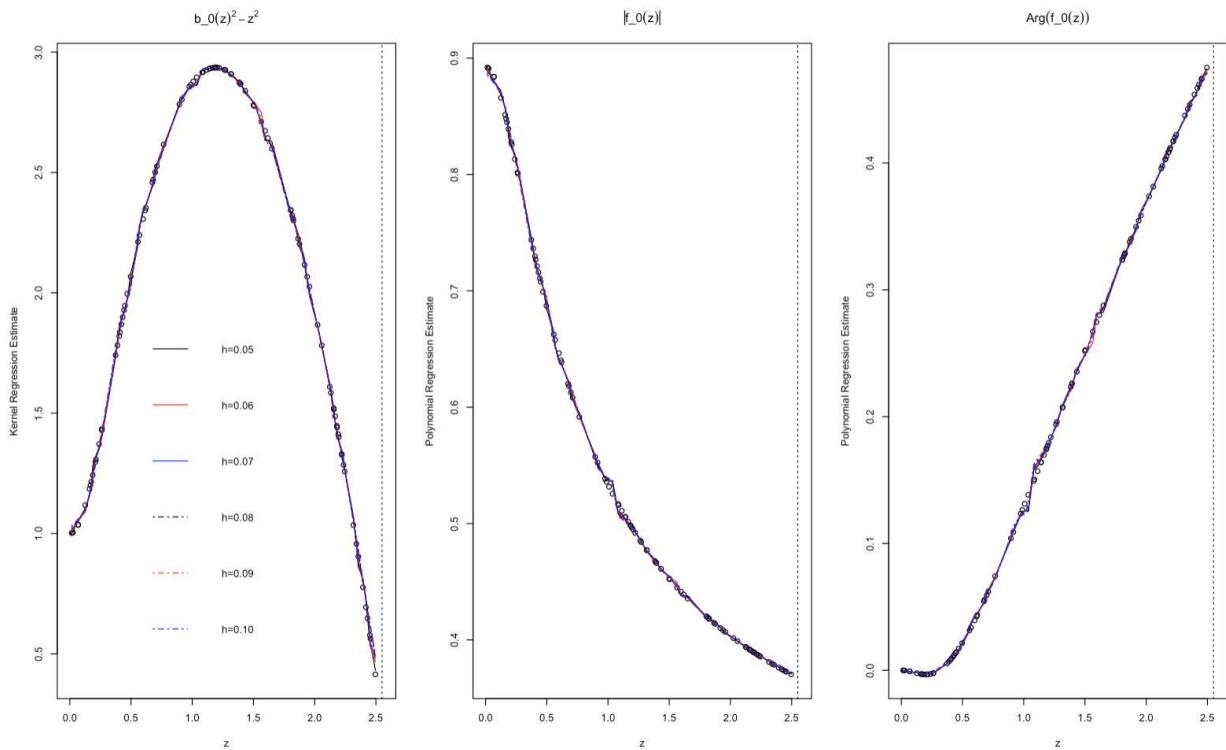
Figure 4. The estimates of critical collapse functions based on a kernel regression method with bandwidth parameters $h = \{0.05, 0.06, 0.07, 0.08, 0.09, 0.10\}$ in elliptic case based on a training sample of size $n = 100$.
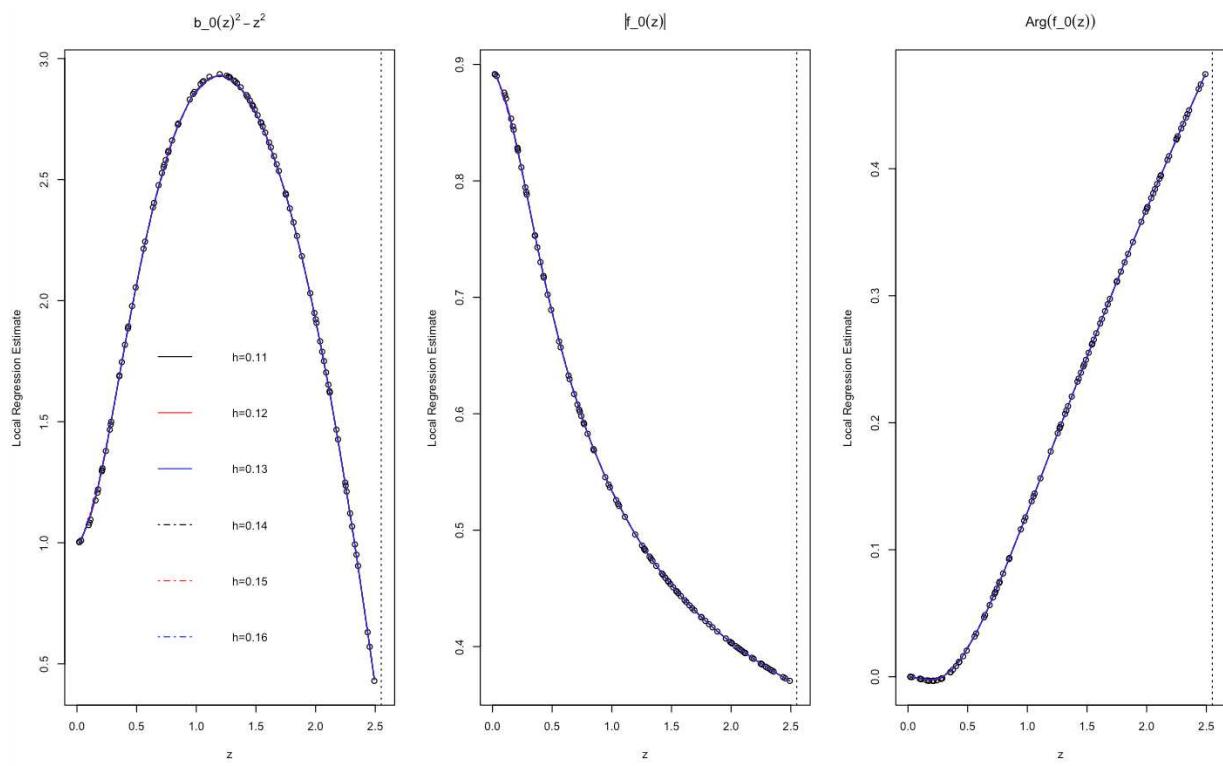
Figure 5. The estimates of critical collapse functions based on a local regression method of order $l = 1$ with bandwidth parameters $h = \{0.11, 0.12, 0.13, 0.14, 0.15, 0.16\}$ in elliptic case based on a training sample of size $n = 100$.
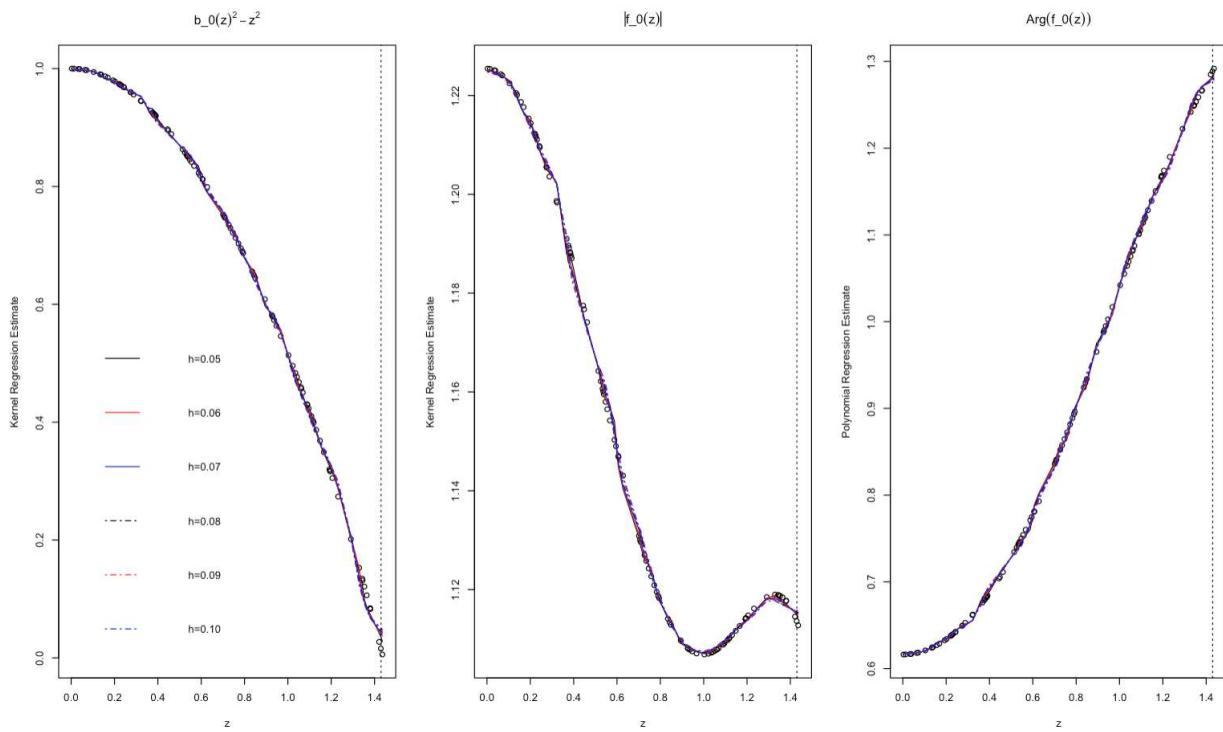
Figure 6. The estimates of critical collapse functions corresponding to an α solution of a hyperbolic case based on a kernel regression method with bandwidth parameters $h = \{0.05, 0.06, 0.07, 0.08, 0.09, 0.10\}$ based on a training sample of size $n = 100$.
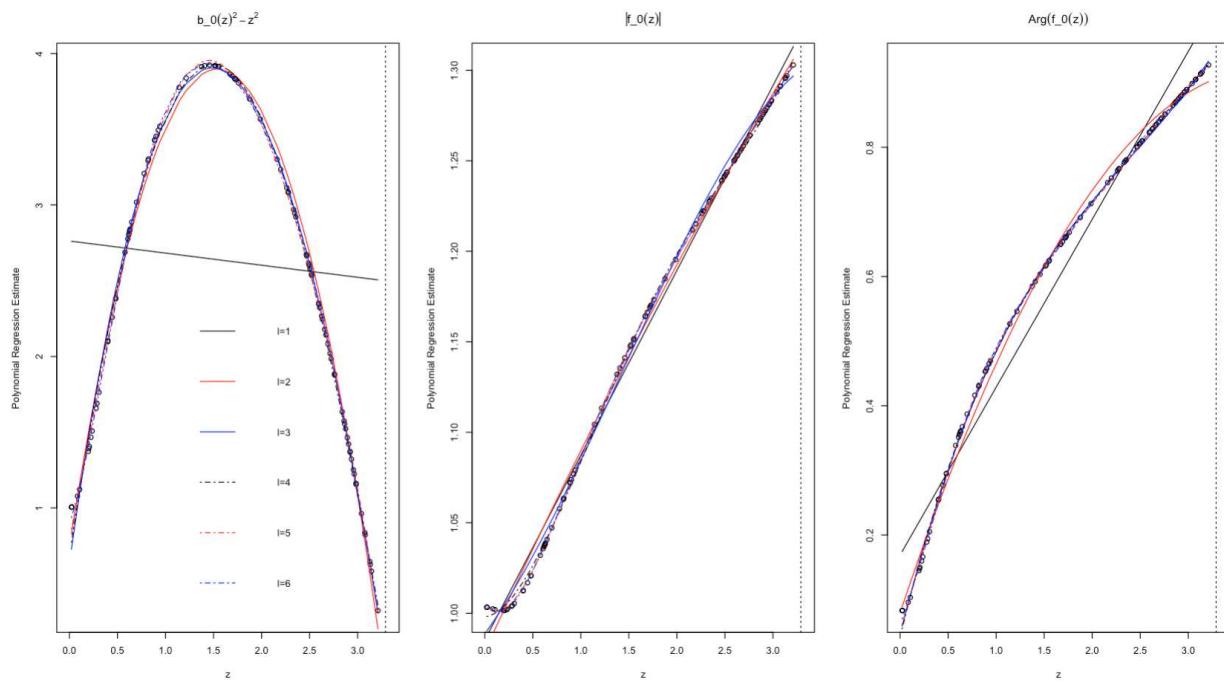
Figure 7. The estimates of critical collapse functions corresponding to a β solution of a hyperbolic case based on a polynomial regression method of orders $l = \{1, \ldots, 6\}$ based on a training sample of size $n = 100$.
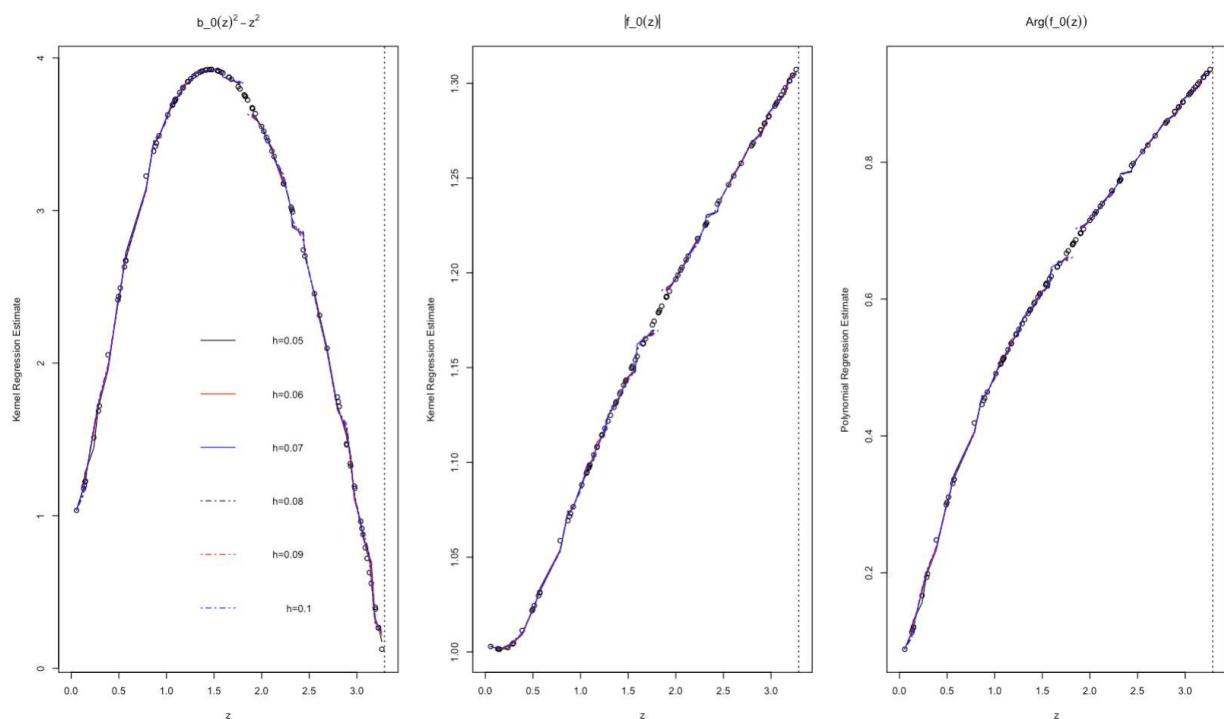
Figure 8. The estimates of critical collapse functions corresponding to a β solution of a hyperbolic case based on a kernel regression method with bandwidth parameters $h = \{0.05, 0.06, 0.07, 0.08, 0.09, 0.10\}$ based on a training sample of size $n = 100$.
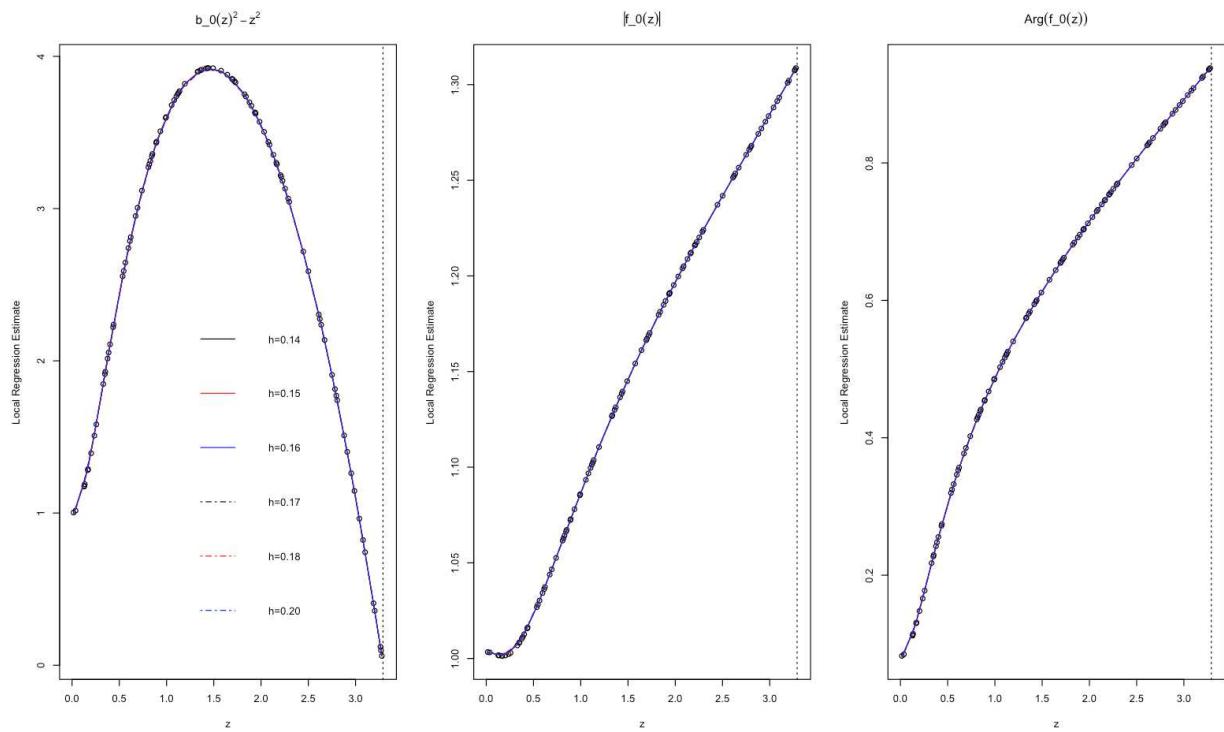
Figure 9. The estimates of critical collapse functions corresponding to a β solution of a hyperbolic case based on a local regression method of order $l = 1$ with bandwidth parameters $h = \{0.14, 0.15, 0.16, 0.17, 0.18, 0.20\}$ based on a training sample of size $n = 100$.
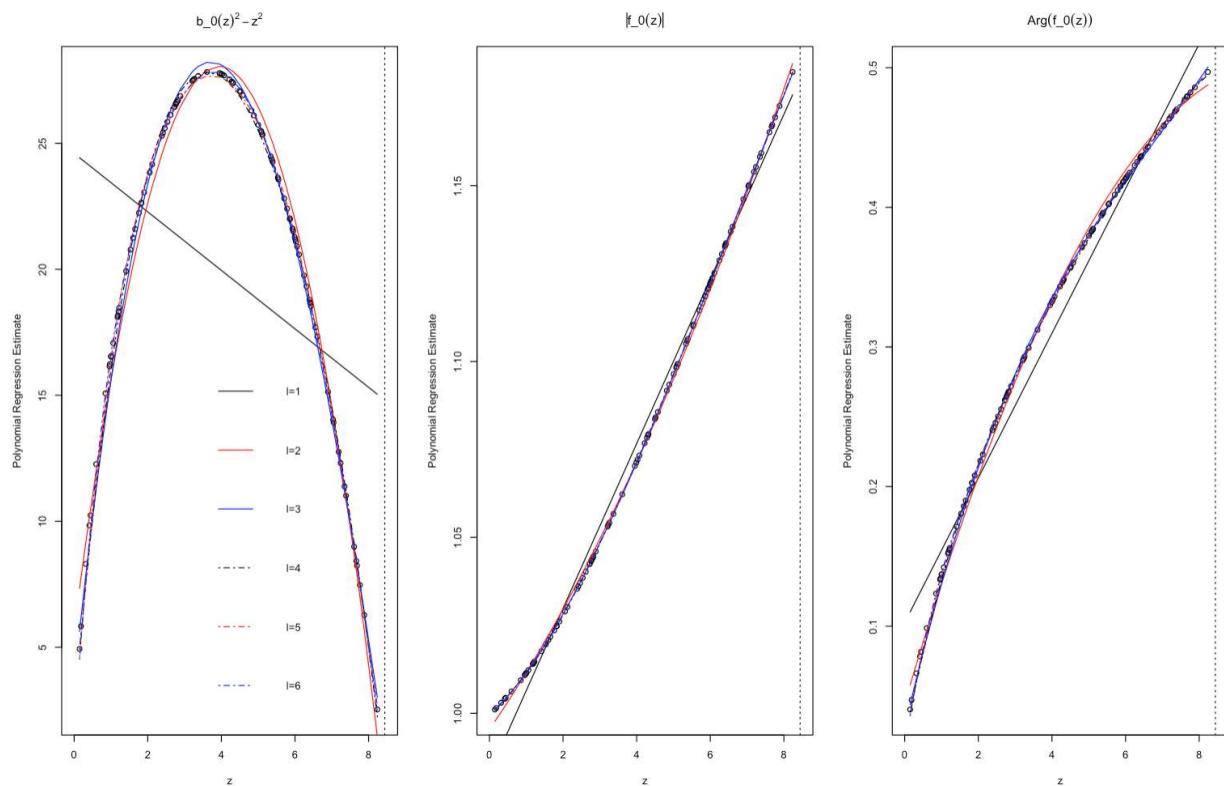

Figure 10. The estimates of critical collapse functions corresponding to a γ solution of a hyperbolic case based on a polynomial regression method of orders $l = \{1, \ldots, 6\}$ based on a training sample of size $n = 100$.
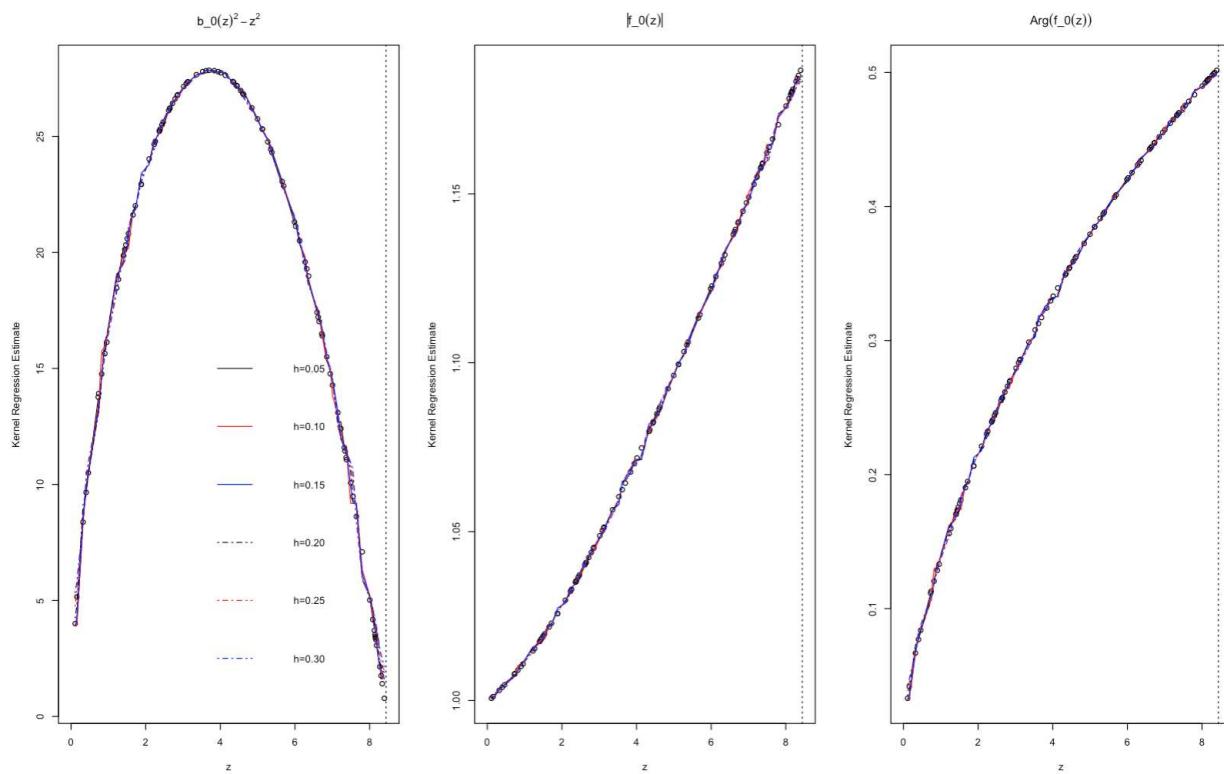
Figure 11. The estimates of critical collapse functions corresponding to a γ solution of a hyperbolic case based on a kernel regression method with bandwidth parameters $h = \{0.05, 0.10, 0.15, 0.20, 0.25, 0.30\}$ based on a training sample of size $n = 100$.
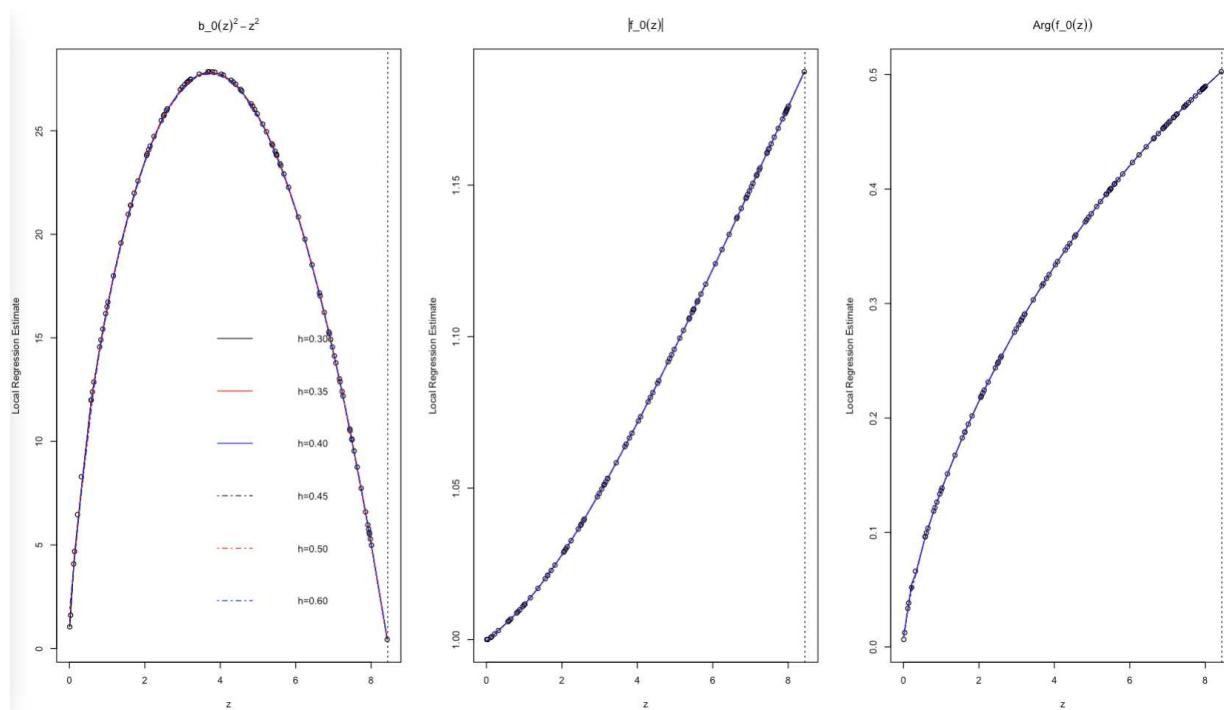

Figure 12. The estimates of critical collapse functions corresponding to a γ solution of a hyperbolic case based on a local regression method of order $l = 1$ with bandwidth parameters $h = \{0.30, 0.35, 0.40, 0.45, 0.50, 0.60\}$ based on a training sample of size $n = 100$.

The local regression estimators outperform the kernel and polynomial counterparts in estimation in almost all three critical collapse functions in both elliptic and hyperbolic do-

mains. This superiority relies on the fact that the local regression estimator takes advantage of polynomial and kernel regression methods in estimation.

While local and kernel regression methods more accurately estimate the critical collapse functions than the polynomial regression method, the polynomial regression method proposes closed form (and continuously differentiable) estimates for the critical functions. These closed and differentiable forms are of high importance to make the critical solutions, critical exponents and the mass of black holes more tractable.

The closed form polynomial regression estimates of order $l = 6$ for critical collapse functions in the elliptic domain are given by

$$\widehat{b_0(z)^2} = 0.9791 + 0.4049z + 8.5099z^2 - 10.6626z^3 + 6.2498z^4 - 1.8050z^5 + 0.2057z^6. \quad (33)$$

$$\widehat{|f_0(z)|} = 0.9010 - 0.2098z - 1.0300z^2 + 1.6785z^3 - 1.1133z^4 + 0.3462z^5 - 0.0414z^6. \quad (34)$$

$$\widehat{\arg f_0(z)} = 0.0037 - 0.1021z + 0.3230z^2 - 0.0578z^3 - 0.0719z^4 + 0.0398z^5 - 0.0060z^6. \quad (35)$$

The closed form polynomial regression estimates of order $l = 6$ for critical collapse functions corresponding to the α-solution domain in hyperbolic space are given by

$$\widehat{b_0(z)^2} = 1.0004 - 0.0138z + 0.5787z^2 - 0.3937z^3 + 0.7078z^4 - 0.4632z^5 + 0.1001z^6. \quad (36)$$

$$\widehat{|f_0(z)|} = 1.2258 - 0.0136z - 0.1681z^2 - 0.3495z^3 + 0.6597z^4 - 0.2450z^5 - 0.0025z^6. \quad (37)$$

$$\widehat{\arg f_0(z)} = 0.6167 - 0.0157z + 0.5834z^2 - 0.5672z^3 + 1.1055z^4 - 0.9240z^5 + 0.2412z^6. \quad (38)$$

The closed form polynomial regression estimates of order $l = 6$ for critical collapse functions corresponding to the β-solution domain in hyperbolic space are given by

$$\widehat{b_0(z)^2} = 0.9051 + 1.9207z + 5.6921z^2 - 6.3768z^3 + 3.1551z^4 - 0.7434z^5 + 0.0678z^6. \quad (39)$$

$$\widehat{|f_0(z)|} = 1.0055 - 0.0828z + 0.3476z^2 - 0.2714z^3 + 0.1069z^4 - 0.0213z^5 + 0.0017z^6. \quad (40)$$

$$\widehat{\arg f_0(z)} = 0.0672 + 0.3845z + 0.3860z^2 - 0.6077z^3 + 0.3346z^4 - 0.0830z^5 + 0.0078z^6. \quad (41)$$

And eventually, the closed form polynomial regression estimates of order $l = 6$ for critical collapse functions corresponding to the γ-solution domain in hyperbolic space are given by

$$\widehat{b_0(z)^2} = 1.9715 + 20.9801z - 7.2930z^2 + 2.2654z^3 - 0.3955z^4 + 0.0350z^5 - 0.0012z^6. \quad (42)$$

$$\widehat{|f_0(z)|} = 0.9997 + 0.0092z + 0.0024z^2 + 0.0001z^3 - 0.0001z^4. \quad (43)$$

$$\widehat{\arg f_0(z)} = 0.0237 + 0.1287z - 0.0204z^2 + 0.0023z^3 - 0.0001z^4. \quad (44)$$

7. Conclusions

The black hole solutions of the axion–dilaton system were recently investigated in elliptic and hyperbolic cases in four and five dimensions [19]. It is crucial for researchers to estimate the functional form of the critical collapse functions. These estimates pave the path to make the critical solutions, critical exponents, the mass of black holes and universality of Choptuik exponents more tractable. To our best knowledge, no research article in the literature investigated the properties of nonlinear statistical models in estimating the critical collapse functions in the Einstein-axion–dilaton system.

In this paper, we employed parametric polynomial regression, non-parametric kernel regression and semi-parametric local polynomial regression for the first time to estimate the functional forms of the critical collapse functions. From numerical studies, we observe

that the local regression estimators outperform the kernel and polynomial counterparts in estimating almost all critical collapse functions in elliptic and hyperbolic domains. While local and kernel methods more accurately estimate the critical collapse function, the polynomial regression method enables us to obtain the closed-form and continuously differentiable estimates for the critical functions. Given the closed forms of critical functions, a pressing question is if one can algebraically derive the critical exponents for the axion–dilaton system. Note that these methods are applied not only for the Einstein-axion–dilaton system and similar solutions but also for other potential systems. These methods are generic and can be used for any matter content for any spacetime dimensions. This is a path that we plan to follow in the near future.

Author Contributions: Methodology, A.H.; Project administration, E.H. All authors have read and agreed to the published version of the manuscript.

Institutional Review Board Statement: Not applicable.

Informed Consent Statement: Not applicable.

Conflicts of Interest: The authors declare no conflict of interest.

References

1. Choptuik, M.W. Universality and Scaling in Gravitational Collapse of a Massless Scalar Field. *Phys. Rev. Lett.* **1993**, *70*, 9. [CrossRef] [PubMed]
2. Gundlach, C. Critical phenomena in gravitational collapse. *Phys. Rep.* **2003**, *376*, 339. [CrossRef]
3. Birukou, M.; Husain, V.; Kunstatter, G.; Vaz, E.; Olivier, M. Scalar field collapse in any dimension. *Phys. Rev. D* **2002**, *65*, 104036. [CrossRef]
4. Husain, V.; Kunstatter, G.; Preston, B.; Birukou, M. Anti-de Sitter gravitational collapse. *Class. Quant. Grav.* **2003**, *20*, L23. [CrossRef]
5. Sorkin, E.; Oren, Y. On Choptuik's scaling in higher dimensions. *Phys. Rev. D* **2005**, *71*, 124005. [CrossRef]
6. Bland, J.; Preston, B.; Becker, M.; Kunstatter, G.; Husain, V. Dimension-dependence of the critical exponent in spherically symmetric gravitational collapse. *Class. Quant. Grav.* **2005**, *22*, 5355. [CrossRef]
7. Rocha, J.V.; Tomašević, M. Self-similarity in Einstein-Maxwell-dilaton theories and critical collapse. *Phys. Rev. D* **2018**, *98*, 104063. [CrossRef]
8. Hirschmann, E.W.; Eardley, D.M. Universal Scaling and Echoing in Gravitational Collapse of a Complex Scalar Field. *Phys. Rev.* **1995**, *D51*, 4198. [CrossRef]
9. Hamade, R.S.; Horne, J.H.; Stewart, J.M. Continuous Self-Similarity and *S*-Duality. *Class. Quant. Grav.* **1996**, *13*, 2241. [CrossRef]
10. Eardley, D.M.; Hirschmann, E.W.; Horne, J.H. S duality at the black hole threshold in gravitational collapse. *Phys. Rev. D* **1995**, *52*, 5397. [CrossRef]
11. Maldacena, J.M. The Large N limit of superconformal field theories and supergravity. *Int. J. Theor. Phys.* **1999**, *38*, 1113–1133. [CrossRef]
12. Witten, E. Anti-de Sitter space and holography. *Adv. Theor. Math. Phys.* **1998**, 2, 253–291. [CrossRef]
13. Gubser, S.; Klebanov, I.R.; Polyakov, A.M. Gauge theory correlators from noncritical string theory. *Phys. Lett. B* **1998**, *428*, 105–114. [CrossRef]
14. Birmingham, D. Choptuik scaling and quasinormal modes in the AdS/CFT correspondence. *Phys. Rev. D* **2001**, *64*, 064024. [CrossRef]
15. Alvarez-Gaume, L.; Gomez, C.; Vazquez-Mozo, M.A. Scaling Phenomena in Gravity from QCD. *Phys. Lett. B* **2007**, *649*, 478. [CrossRef]
16. Hatefi, E.; Nurmagambetov, A.; Park, I. ADM reduction of IIB on $\mathcal{H}^{p,q}$ to dS braneworld. *JHEP* **2013**, *4*, 170. [CrossRef]
17. Hatefi, E.; Nurmagambetov, A.J.; Park, I.Y. N^3 entropy of $M5$ branes from dielectric effect. *Nucl. Phys. B* **2013**, *866*, 58–71. [CrossRef]
18. de Alwis, S.; Gupta, R.; Hatefi, E.; Quevedo, F. Stability, Tunneling and Flux Changing de Sitter Transitions in the Large Volume String Scenario. *JHEP* **2013**, *11*, 179. [CrossRef]

19.   Antonelli, R.; Hatefi, E. On self-similar axion-dilaton configurations. *JHEP* **2020**, *3*, 74. [CrossRef]
20.   Antonelli, R.; Hatefi, E. On Critical Exponents for Self-Similar Collapse. *JHEP* **2020**, *3*, 180. [CrossRef]
21.   Hatefi, E.; Vanzan, E. On higher dimensional self-similar axion–dilaton solutions. *Eur. Phys. J. C* **2020**, *80*, 952. [CrossRef]
22.   Hatefi, E.; Kuntz, A. On Perturbation Theory and Critical Exponents for Self-Similar Systems. *Eur. Phys. J. C* **2021**, *81*, 15. [CrossRef]
23.   Hamade, R.S.; Stewart, J.M. The spherically symmetric collapse of a massless scalar field. *Class. Quant. Grav.* **1996**, *13*, 497. [CrossRef]
24.   Abrahams, A.M.; Evans, C.R. Critical Behavior and Scaling in Vacuum Axisymmetric Gravitational Collapse. *Phys Rev. Lett.* **1993**, *70*, 2980. [CrossRef] [PubMed]
25.   Evans, C.R.; Coleman, J.S. Critical Phenomena and Self-Similarity in the Gravitational Collapse of Radiation Fluid. *Phys. Rev. Lett.* **1994**, *72*, 1782. [CrossRef] [PubMed]
26.   Koike, T.; Hara, T.; Adachi, S. Critical behavior in gravitational collapse of radiation fluid: A Renormalization group (linear perturbation) analysis. *Phys. Rev. Lett.* **1995**, *74*, 5170. [CrossRef]
27.   Maison, D. Nonuniversality of critical behavior in spherically symmetric gravitational collapse. *Phys. Lett. B* **1996**, *366*, 82. [CrossRef]
28.   Sen, A. Strong-weak coupling duality in four-dimensional string theory. *Int. J. Mod. Phys. A* **1994**, *9*, 3707. [CrossRef]
29.   Schwarz, J.H. Evidence for nonperturbative string symmetries. *Lett. Math. Phys.* **1995**, *34*, 309. [CrossRef]
30.   Álvarez-Gaumé, L.; Hatefi, E. Critical Collapse in the Axion-Dilaton System in Diverse Dimensions. *Class. Quant. Grav.* **2012**, *29*, 025006. [CrossRef]
31.   Green, M.B.; Schwarz, J.H.; Witten, E. *Superstring Theory*; Cambridge University Press: Cambridge, UK, 1987; Volumes 1 and 2.
32.   Polchinski, J. *String Theory*; Cambridge University Press: Cambridge, UK, 1998; Volumes 1 and 2.
33.   Font, A.; Ibanez, L.E.; Lust, D.; Quevedo, F. Strong-weak coupling duality and nonperturbative effects in string theory. *Phys. Lett. B* **1990**, *249*, 35. [CrossRef]
34.   Álvarez-Gaumé, L.; Hatefi, E. More On Critical Collapse of Axion-Dilaton System in Dimension Four. *JCAP* **2013**, *1310*, 37. [CrossRef]
35.   Hirschmann, E.W.; Eardley, D.M. Criticality and bifurcation in the gravitational collapse of a selfcoupled scalar field. *Phys. Rev. D* **1997**, *56*, 4696–4705. [CrossRef]
36.   Harrell, F.E., Jr. *Regression Modeling Strategies: With Applications to Linear Models, Logistic and Oordinal Regression, and Survival Analysis*; Springer: Berlin/Heidelberg, Germany, 2015.
37.   Cleveland, W.S.; Loader, C. Smoothing by local regression: Principles and methods. In *Statistical Theory and Computational Aspects of Smoothing*; Physica-Verlag: Heidelberg, Germany, 1996.
38.   Nadaraya, E.A. On estimating regression. *Theory Probab. Its Appl.* **1964**, *9*, 141–142. [CrossRef]
39.   Watson, G.S. Smooth regression analysis. *Sankhyā Indian J. Stat. Ser.* **1964**, *26*, 359–372.